Combining Cauchy and characteristic codes. V. Cauchy-characteristic matching for a spherical spacetime containing a perfect fluid

Mark R. Dubal, Ray A. d'Inverno, and James A. Vickers
Faculty of Mathematical Studies, University of Southampton, Southampton SO17 1BJ, United Kingdom
(Received 5 March 1998; published 24 July 1998)

This paper is part of a long term program to develop CCM (combined Cauchy and characteristic) codes as investigative tools in numerical relativity. The approach has two distinct features: (i) it dispenses with an outer boundary condition and replaces this with matching conditions at an interface between the Cauchy and characteristic regions, and (ii) by employing a compactified coordinate, it proves possible to generate global solutions. In this paper it is shown that CCM can be used effectively to model a spherically symmetric perfect fluid. A particular advantage of CCM in avoiding arbitrary mass inflow-outflow boundary conditions is pointed out. Results are presented which include fluid distributions which form black holes and those which give rise to mass outflow. [S0556-2821(98)06516-3]

PACS number(s): 04.25.Dm, 04.20.Ha, 04.40.Nr, 04.70.Bw

I. INTRODUCTION

Cauchy-characteristic matching (CCM) is a technique which replaces the *ad hoc* boundary conditions at the edge of a finite numerical grid by a compactified characteristic region. The characteristic region provides the correct behavior for waves at the boundary. Information is passed between the inner and outer grids via an interface region which takes account of coordinate transformations [1].

In recent years CCM has been applied to a number of problems, particularly scalar fields [2] and cylindrical gravitational waves [3] with work on axisymmetric gravitational waves in progress [4]. A notable exception is its application to spacetimes containing a perfect fluid. Since this is one of the most important sources in astrophysics, an investigation using CCM would be very interesting. Indeed it could provide a way of dealing with other boundary problems which arise in fluid spacetimes, but are absent in scalar field and gravitational wave spacetimes. Some previous works have looked at incorporating matter, usually dust [5] or radiation fluid [6], into purely characteristic codes. These have been in the context of cosmology and critical behavior respectively and so have not used a compactified coordinate system. A particular problem with this approach, especially when matter is present, is the appearance of caustics which require special treatment if they are not to halt the numerical code. Careful use of CCM can circumvent this difficulty by confining the large density, strong field dynamics to the inner Cauchy region. Moreover purely characteristic formulations often have stability problems at $r=0$ which are avoided with CCM.

When modelling spacetimes with a perfect fluid a number of numerical methods can be used. Particle type hydrodynamics is possible [7], where the fluid is followed in a Lagrangian manner. This would appear to avoid outer boundary problems; the main difficulty can be the loss of accuracy when the fluid becomes very dispersed. The more traditional finite-difference and finite-element approaches usually use an Eulerian type scheme where the fluid moves across a grid (which may or may not be moving itself). For one-dimensional problems it is quite easy to follow the fluid-vacuum interface and apply boundary conditions there. In higher dimensions, however, such an approach becomes extremely difficult. Normally the initial fluid distribution is set up near the center of the grid while the ''vacuum'' region is filled with a very low density material [8]. The boundary conditions are then fixed at the edge of the grid. This can be satisfactory if the grid is sufficiently large that significant amounts of fluid never reach the boundary, but it does introduce a number of difficulties which CCM can address.

First, as in the case of a scalar field or gravitational waves, the outer boundary is an artificial one and can give rise to spurious reflections of waves which in time can seriously affect the numerical evolution. This is the problem that CCM usually deals with. In the fluid case there is a second difficulty. There is an arbitrary inflow-outflow boundary at the edge of the grid. To avoid significant mass changes the grid must be large enough to ensure that the density is always very low near the boundary. This can mean a very large grid for something like the simulation of super-nova explosions. Since one of the main advantages of CCM is to make a large grid for gravitational wave extraction unnecessary, it would be useful to be able to use a small grid even if fluid is present. This is the goal of the current work.

In this paper we investigate CCM for a spherical spacetime with a perfect fluid. The inner Cauchy portion of the calculation uses a standard Arnowitt-Deser-Misner (ADM) $3+1$ approach [9] and is described quite briefly. Here we concentrate on the details of the characteristic region and on the interface. In particular we look at the asymptotic behavior of the fluid density and energy which is required to have a finite mass at future-null-infinity. The interface conditions which match the Cauchy portion (using a radial gauge with polar time slicing) to the characteristic region (using Bondi coordinates) are described in detail. Results from a number of runs of the code are shown. They include fluid distributions which form black holes and those which give rise to mass outflow. The code is shown to be second-order convergent and stable over long periods of time.

II. CAUCHY EINSTEIN EQUATIONS

In the following $c=G=1$ and the spacetime metric has the signature $(-,+,+,+)$ and spacetime tensor indices are denoted by lowercase Greek letters (e.g. μ, ν, ...).

We list here the equations for the Cauchy portion of the code. These are obtained using standard ADM $3+1$ methods on the Einstein equations [9], the divergence of the stress-energy tensor and baryon conservation. A radial gauge is used for which the spherically symmetric line element is

$$ds^2=-\alpha^2(r,t)dt^2+a^2(r,t)dr^2+r^2d\Omega^2, \tag{1}$$

where r is such that $A=4\pi r^2$ is the proper area of a spherical surface at coordinate distance r from the origin, $d\Omega^2$ is the flat metric on S^2, a is the radial metric function and α is the lapse function. The lapse function will be determined by imposing the polar time-slicing condition [10]

$$K^{\theta}_{\theta}+K^{\phi}_{\phi}=0. \tag{2}$$

The stress-energy tensor of the perfect fluid is given by

$$T_{\mu\nu}=\rho_* w v_\mu v_\nu+pg_{\mu\nu}, \tag{3}$$

where ρ_*, $w=1+e+p/\rho_*$ and p are, respectively, the rest mass density, the relativistic enthalpy and the thermal pressure, all measured in the fluid co-moving frame. The quantity e is the specific internal energy and v^μ is the fluid 4-velocity. Given the metric (1) and the stress-energy tensor (3) the set of equations to be solved is

$$D_{,t}+\frac{1}{r^2}(r^2DV^r)_{,r}=0 \tag{4}$$

$$E_{,t}+\frac{1}{r^2}[r^2(E+p)V^r]_{,r}=0 \tag{5}$$

$$Z_{,t}+\frac{1}{r^2}[r^2(ZV^r+\alpha ap)]_{,r}-\frac{\alpha}{a^2}ZUa_{,r}$$

$$+a(E+p)\alpha_{,r}-\frac{p}{r^2}(r^2\alpha a)_{,r}=0 \tag{6}$$

$$\frac{\alpha_{,r}}{\alpha}-\frac{a^2-1}{2r}-4\pi r(a^2p+ZU)=0, \tag{7}$$

$$\frac{a_{,r}}{a}+\frac{a^2-1}{2r}-4\pi ra^2E=0 \tag{8}$$

supplemented by the equation of state

$$p=(\Gamma-1)\rho_* e. \tag{9}$$

Note that this system is more general than that of a radiation fluid, where the evolution equation for e would not need to be considered. However it is required for a consistent treatment of shocks. In the above $V^r=v^r/v^t=\alpha U/a$ is the local 3-velocity of the fluid, Γ is the adiabatic index and the dynamical fluid variables have been defined as

$$D=\rho_* a\alpha v^t, \tag{10}$$

$$E=\rho_* w(\alpha v^t)^2-p, \tag{11}$$

$$Z=\rho_* wa^2(\alpha v^t)^2U. \tag{12}$$

The pressure can be obtained from the fundamental variables and the equation of state via the implicit equation

$$X=\left\{\left(\frac{aX}{(\gamma-1)D}\right)^2\left[\gamma E-X-\frac{(\gamma-1)}{X}\left(\frac{Z}{a^2}\right)^2\right]^2+\left(\frac{Z}{a^2}\right)^2\right\}^{1/2} \tag{13}$$

where $X=E+p$. The 3-velocity can then be found as

$$V^r=\frac{\alpha Z}{a^3(E+p)}=\frac{\alpha}{a}U. \tag{14}$$

III. CHARACTERISTIC EINSTEIN EQUATIONS

On the characteristic side we use a Bondi coordinate system. Bondi's line element for an axially symmetric spacetime possessing azimuth-reflection invariance with signature $(-,+,+,+)$ is [11]

$$ds^2=-(Ve^{2\beta}/\tilde{r}-\tilde{r}^2U^2e^{2\gamma})du^2-2e^{2\beta}dud\tilde{r}$$

$$-2\tilde{r}^2Ue^{2\gamma}dud\theta+\tilde{r}^2e^{2\gamma}d\theta^2+\tilde{r}^2e^{-2\gamma}\sin^2\theta d\phi^2, \tag{15}$$

where V, U, β and γ are all functions of $(u,\tilde{r},\theta)$. If we make the additional assumption that the line element is spherically symmetric, then Eq. (15) reduces to the form (see Appendix A)

$$ds^2=-\frac{Ve^{2\beta}}{\tilde{r}}du^2-2e^{2\beta}dud\tilde{r}+\tilde{r}^2d\Omega^2, \tag{16}$$

where $V=V(u,\tilde{r})$ and $\beta=\beta(u,\tilde{r})$ only.

The assumption of spherical symmetry means that in the characteristic region the fluid 4-velocity has components

$$v^\mu=(v^u,\ v^{\tilde{r}},\ 0,\ 0), \tag{17}$$

where the fluid variables v^u, $v^{\tilde{r}}$, p, ρ_* and e are all functions of $(u,\tilde{r})$ only. The normalizing condition

$$v^\mu v_\mu=-Ve^{2\beta}(v^u)^2/\tilde{r}-2e^{2\beta}v^uv^{\tilde{r}}=-1 \tag{18}$$

then enables us to eliminate $v^{\tilde{r}}$ in terms of metric variables and v^u, since $v^u\neq 0$. In addition, the equation of state (9) enables us to eliminate p, in which case there are three remaining independent physical variables, namely e, ρ_* and v^u.

Defining the field equations in terms of

$$E_{\mu\nu} \equiv G_{\mu\nu} - 8\pi T_{\mu\nu} = 0, \tag{19}$$

then

$$L^1 \equiv E_{11} = 0 \quad \text{determines} \quad \beta_{,\tilde{r}}, \tag{20}$$

$$L^2 \equiv 2g^{01}E_{11} + g^{11}E_{11} = 0 \quad \text{determines} \quad V_{,\tilde{r}}, \tag{21}$$

$$L^3 \equiv E_{22} = 0 \quad \text{determines} \quad (\beta_{,\tilde{r}})_{,u}, \tag{22}$$

where all the other quantities in the three equations are known at each stage of the integration. In addition,

$$E_{00} = 0 \quad \text{determines} \quad V_{,u}. \tag{23}$$

We use this last equation to eliminate null derivatives of the metric variable V from subsequent equations. Then the conservation equations

$$T^{\mu\nu}{}_{;\nu} = 0, \tag{24}$$

together with the equation of baryon conservation

$$(\rho_* v^\mu)_{;\mu} = 0, \tag{25}$$

provide three equations which between them determine the null derivatives of the three physical variables e, ρ_* and v^u. Specifically, after substitution,

$$L^4 \equiv T^{u\mu}{}_{;\mu} = 0 \quad \text{determines} \quad e_{,u}, \tag{26}$$

$$L^5 \equiv (\rho_* u^\mu)_{;\mu} = 0 \quad \text{determines} \quad \rho_{*,u}, \tag{27}$$

$$L^6 \equiv T^{\tilde{r}\mu}{}_{;\mu} = 0 \quad \text{determines} \quad v^u{}_{,u}, \tag{28}$$

where all the other quantities in the three equations are known at each stage of the integration.

We next introduce a compactified radial coordinate

$$y = 1/\tilde{r}, \tag{29}$$

define

$$\mathcal{B} = \beta_{,u}, \tag{30}$$

and replace V with the function

$$W = V - e^{2\beta}/y, \tag{31}$$

which remains finite at null infinity. The resulting line element is

$$ds^2 = -(We^{2\beta}y + e^{4\beta})du^2 + \frac{2e^{2\beta}}{y^2}dudy + \frac{1}{y^2}d\Omega^2. \tag{32}$$

In these new coordinates, the three equations $L^1 = L^2 = L^3 = 0$ for determining the metric become, respectively,

$$\beta_{,y} = -2\pi y S (v^u)^2 e^{4\beta}(1 + \Gamma e), \tag{33}$$

$$W_{,y} = 4\pi S e^{2\beta}[(v^u)^2 e^{4\beta}(1 + \Gamma e) + e(2 - \Gamma)] \tag{34}$$

and

$$\mathcal{B}_{,y} = AS_{,y} + B(v^u)_{,y} + Ce_{,y} + D + E, \tag{35}$$

where

$$S = \rho_* / y^4, \tag{36}$$

and

$$A = \pi y^3 e^{2\beta}[e^{2\beta}(v^u)^2(e\Gamma + 1)(yW + e^{2\beta}) + (e\Gamma - 2e - 1)],$$

$$B = 2\pi y^3 (e\Gamma + 1) v^u e^{4\beta} SF,$$

$$C = \pi y^3 e^{2\beta} S[\Gamma (v^u)^2 e^{2\beta} F + \Gamma - 2],$$

$$D = 8\pi y^4 e^{6\beta}(v^u)^2 S^2[(2e + 2e^2\Gamma - e^2\Gamma^2 + 1) - (1 + 2e\Gamma + e^2\Gamma^2)(v^u)^2 e^{2\beta} F],$$

$$E = 2\pi y^2 e^{2\beta} S[(v^u)^2 e^{2\beta}(1 + e\Gamma)(e^{2\beta} + 2yW) + (3e\Gamma - 4e - 1)],$$

$$F = yW + e^{2\beta}.$$

The three equations $L^4 = L^5 = L^6 = 0$ for determining the evolution of the three independent physical variables become

$$S_{,u} = [y^2 BS_{,y} + ySC - y^2 SD(v^u)_{,y} + y^2 Ee_{,y}]/A, \tag{37}$$

where

$$A = (1 + 2e\Gamma - e\Gamma^2)(v^u)^2,$$

$$B = (e\Gamma^2 - 2e\Gamma - 1)F/2 + e(\Gamma - 1)e^{-2\beta},$$

$$C = (2e\Gamma^2 - 3e\Gamma - 1)F + 4e(\Gamma - 1)e^{-2\beta},$$

$$D = (e\Gamma + 1)e^{-2\beta}/v^u,$$

$$E = S(\Gamma - 1)e^{-2\beta},$$

$$F = [yW(v^u)^2 + e^{2\beta}(v^u)^2 - e^{-2\beta}]$$

for the density,

$$e_{,u} = [y^2 eBS_{,y} + yeSC - y^2 eD(v^u)_{,y} + y^2 SEe_{,y}]/A, \tag{38}$$

where

$$A = (1 + 2e\Gamma - e\Gamma^2)S(v^u)^2,$$

$$B = e(\Gamma^2 - 2\Gamma + 1)e^{-2\beta},$$

$$C = FG + 2(e\Gamma^2 - 3e\Gamma - \Gamma + 1 + 2e)e^{-2\beta},$$

$$D = SFe^{-2\beta}/v^u,$$

$$E = (e\Gamma^2 - 2e\Gamma - 1)G/2 + (1 + e)e^{-2\beta},$$

$$F=(e\Gamma^2-e\Gamma+\Gamma-1),$$

$$G=[yW(v^u)^2+e^{2\beta}+e^{-2\beta}],$$

for the specific internal energy, and

$$v^u_{,u}=[-y^2B(eS)_{,y}+y^2SC(v^u)_{,y}+SD-2\pi y^3S^2e^{2\beta}E]/A, \tag{39}$$

where

$$A=(1+2e\Gamma-e\Gamma^2)S(v^u)^2,$$

$$B=(\Gamma-1)e^{-2\beta},$$

$$C=(e\Gamma^2-2e\Gamma-1)Fv^u/2+(e\Gamma^2+1)e^{-2\beta}/2v^u,$$

$$D=2\mathcal{B}(e\Gamma^2-2e\Gamma-1)(v^u)^2-y^2W(e\Gamma^2+1)(v^u)^2/2$$
$$+ye\Gamma e^{-2\beta}(1-\Gamma)(v^u)^2+ye(\Gamma^2-5\Gamma+4)e^{-2\beta},$$

$$E=[yE(v^u)^2e^{2\beta}+(v^u)^2e^{4\beta}+1]$$
$$\times(e^2\Gamma^3-2e^2\Gamma^2+e\Gamma^2-3e\Gamma-1)$$
$$+2(2e^2\Gamma-e^2\Gamma^2-e\Gamma^2+e+2e\Gamma+1),$$

$$F=yW+e^{2\beta}$$

for the zeroth component of the fluid 4-velocity. The numerical integration scheme for these and the Cauchy equations (4)–(8) is described in Sec. VI.

IV. INTERFACE MATCHING

The two line elements we wish to relate are given in (t,r,θ,ϕ) Cauchy coordinates by

$$ds^2=-\alpha^2(r,t)dt^2+a^2(r,t)dr^2+r^2(d\theta^2+\sin^2\theta d\phi^2), \tag{40}$$

and in $(u,\tilde{r},\tilde{\theta},\tilde{\phi})$ Bondi coordinates by

$$ds^2=-A(\tilde{r},u)du^2-2B(\tilde{r},u)d\tilde{r}du+\tilde{r}^2(d\tilde{\theta}^2+\sin^2\tilde{\theta}d\tilde{\phi}^2). \tag{41}$$

The quantities A and B are given in the Bondi parametrization of the metric by

$$A=Ve^{2\beta}/\tilde{r}, \tag{42}$$

$$B=e^{2\beta}. \tag{43}$$

In this section it is more convenient to work with A and B rather than V (or W) and β, although Appendix B gives the results in terms of the variables used for the numerical code. Because of the spherical symmetry, we may take $\tilde{\theta}=\theta$ and $\tilde{\phi}=\phi$. Since the transformation between (t,r) and $(u,\tilde{r})$ is independent of the angular variables a comparison between Eqs. (40) and (41) shows us we must have

$$\tilde{r}=r. \tag{44}$$

Note however that we will retain the tilde in this section to distinguish between $\partial/\partial r$ and $\partial/\partial\tilde{r}$. Because of the spherical symmetry, we may write

$$u=f(r,t). \tag{45}$$

Differentiating this gives

$$-Adu^2-2Bdud\tilde{r}=-Af_{,t}^2dt^2-2f_{,t}(Af_{,r}+B)dtdr$$
$$-(Af_{,r}^2+2Bf_{,r})dr^2. \tag{46}$$

Comparing with Eq. (40) we see that

$$\alpha^2=Af_{,t}^2, \tag{47}$$

$$0=f_{,t}(Af_{,r}+B), \tag{48}$$

$$-a^2=Af_{,r}^2+2Bf_{,r}. \tag{49}$$

Since we do not want $f_{,t}=0$, Eq. (48) gives

$$f_{,r}=-BA^{-1}, \tag{50}$$

and substituting in Eq. (49) gives

$$a^2=B^2A^{-1}. \tag{51}$$

To calculate α^2 we need to know $f_{,t}$. We choose to label the null hypersurfaces so that u and t agree on the interface at radius $r=r_0$. Thus

$$f(r_0,t)=t, \tag{52}$$

and hence

$$f_{,t}(r_0,t)=1. \tag{53}$$

Substituting this in Eq. (47) gives

$$\alpha^2(r_0,t)=A(r_0,t). \tag{54}$$

Note that Eq. (54) is valid only on the interface whereas Eq. (51) is valid everywhere.

We also need to calculate how the derivatives of the metric coefficients are related. Since the angular and time variables for the two coordinate systems agree on the interface, we may calculate these derivatives by differentiating Eqs. (51) and (54). Also since Eq. (51) is valid everywhere, we may calculate the radial derivative of a using the chain rule to obtain

$$a_{,r}=(BA^{-1/2})_{,\tilde{r}}-BA^{-1}(BA^{-1/2})_{,u}. \tag{55}$$

Similarly differentiating Eq. (47) gives

$$\alpha_{,r}=(A^{1/2})_{,\tilde{r}}f_{,t}-BA^{-1}(A^{1/2})_{,u}f_{,t}+A^{1/2}f_{,tr}. \tag{56}$$

But, by Eq. (48),

$$f_{,tr}=-f_{,t}(BA^{-1})_{,u}. \tag{57}$$

Using $f_{,t}=1$ on the interface we obtain

$$\alpha_{,r} = (A^{1/2})_{,\tilde{r}} - (BA^{-1/2})_{,u} \quad \text{on} \quad r = r_0. \tag{58}$$

The matter variables ρ_* and e are scalars and therefore agree on the interface, as do their angular and time derivatives. The radial derivatives are related by the chain rule

$$\Phi_{,r} = \Phi_{,\tilde{r}} - BA^{-1}\Phi_{,u}. \tag{59}$$

The transformation of the 4-velocity v^μ is given by

$$v^{\tilde{r}} = v^r, \tag{60}$$

$$v^u = f_{,t}v^t + f_{,r}v^r. \tag{61}$$

Taking $r = r_0$ and solving for v^t and v^r gives

$$v^r = v^{\tilde{r}}, \tag{62}$$

$$v^t = v^u + BA^{-1}v^{\tilde{r}}. \tag{63}$$

As with the metric coefficients we also require the relationship between the derivatives. Taking the radial derivative of Eq. (60) using the chain rule gives

$$v^r_{,r} = v^{\tilde{r}}_{,\tilde{r}} - (BA^{-1})^{\tilde{r}}_{,u}. \tag{64}$$

Similarly taking the radial derivative of Eq. (61) gives

$$v^u_{,r} = f_{,tr}v^t + f_{,rr}v^r + f_{,t}v^t_{,r} + f_{,r}v^r_{,r}. \tag{65}$$

Using Eq. (57) to substitute for $f_{,tr}$, differentiating Eq. (50) to find $f_{,rr}$, and calculating $v^u_{,r}$ using the chain rule yields

$$\begin{aligned} v^t_{,r} &= v^u_{,\tilde{r}} - BA^{-1}v^u_{,u} + BA^{-1}v^{\tilde{r}}_{,\tilde{r}} - B^2A^{-2}v^{\tilde{r}}_{,u} \\ &= (BA^{-1})_{,u}v^u + (BA^{-1})_{,\tilde{r}}v^{\tilde{r}}. \end{aligned} \tag{66}$$

Thus Eqs. (51), (54), (55), (58), (62), (63), (64) and (66) give the metric variables, matter variables and their radial derivatives in the Cauchy region in terms of the corresponding quantities in the Bondi region. A very similar calculation gives the inverse transformation. The final formulas are given in Appendix B.

V. FLUID BEHAVIOR AT NULL INFINITY

In Newtonian theory stars are often described as static polytropic gas spheres with equation of state $p = K\rho^\Gamma$. A solution of considerable interest is the case $\Gamma = 6/5$ for which the matter extends to infinity, but the total mass is finite. A relativistic analogue of this solution was obtained by Buchdahl [12]. The initial data we evolve numerically will consist of the Buchdahl solution perturbed by a Gaussian pulse. Buchdahl originally gave his solution in isotropic coordinates as

$$ds^2 = e^\nu dt^2 - e^{-\mu}(dR^2 + R^2 d\Omega^2) \tag{67}$$

where

$$e^\nu = (1-f)^2(1+f)^{-2}, \tag{68}$$

$$e^\mu = (1+f)^4, \tag{69}$$

$$f = \frac{a}{2}(1+kR^2)^{-1/2}. \tag{70}$$

This solution represents a static fluid with pressure p and density ρ given by

$$p = bf^6(1+f)^{-5}(1-f), \tag{71}$$

$$\rho = 3bf^5(1+f)^{-5}, \tag{72}$$

$$b = 8k/(a^4\pi). \tag{73}$$

This is not an exact polytrope as p is related to ρ by

$$p = \frac{\rho^{6/5}}{1+2q_c(1-\rho^{1/5})}, \quad q_c = \left(\frac{3p}{\rho}\right)_{\text{center}}; \tag{74}$$

however, the density falls off like r^{-5}, and so this is close to an exact polytropic equation of state in the asymptotic region. Note that p and ρ are related to our choice of matter variables ρ_* and e by

$$p = (\Gamma - 1)\rho_* e, \tag{75}$$

$$\rho = (1+e)\rho_*. \tag{76}$$

Since the solution is static, the 4-velocity of the fluid is given by

$$v^t = (1+f)(1-f)^{-1}, \tag{77}$$

$$v^a = 0 \quad \text{otherwise}. \tag{78}$$

The purpose of this section is to find the asymptotic behavior of the Buchdahl solution in Bondi coordinates. We start by noting that

$$f = \frac{c}{R} + O(R^{-3}) \quad \text{where} \quad c = \frac{a}{2\sqrt{k}}, \tag{79}$$

which enables us to calculate the asymptotic behavior of the various quantities in terms of the isotropic radius coordinate R. The next step is to convert the metric to the radial gauge coordinate system used in the Cauchy region. The radial gauge r coordinate is related to the isotropic R coordinate system by

$$r^2 = (1+f)^4 R^2, \tag{80}$$

so that

$$r = R + 2c + \frac{c^2}{R^2} + O(R^{-3}). \tag{81}$$

This gives

$$e^\nu = 1 - 4c/r + (8c^2 + 4ac)/r^2 + O(r^{-3}), \tag{82}$$

$$e^\mu = 1 + 4c/r + (6c^2 - 4ac)/r^2 + O(r^{-3}), \tag{83}$$

$$dR^2=[1+2c^2/r^2+O(r^{-3})]dr^2. \tag{84}$$

Equating Eq. (67) with Eq. (1) gives

$$\alpha^2=1-4c/r+(8c^2+4ac)/r^2+O(r^{-3}), \tag{85}$$

$$a^2=1+4c/r+(8c^2-4ac)/r^2+O(r^{-3}). \tag{86}$$

We now change to Bondi coordinates. As we have seen in the previous section the transformation between Cauchy and Bondi coordinates is not straightforward in general. However, in the special case of a static solution which we are considering here it is possible to obtain transformation formulas which are valid everywhere and not just at the interface. These give

$$A=\alpha^2, \tag{87}$$

$$B=\alpha a, \tag{88}$$

which by Eqs. (85),(86) give

$$A=1-4c/r+(8c^2+4ac)/r^2+O(r^{-3}), \tag{89}$$

$$B=1+O(r^{-3}). \tag{90}$$

In terms of the Bondi parametrization this is equivalent to

$$\beta=O(r^{-3}), \tag{91}$$

$$V=r-4c+(8c^2+4ac)/r+O(r^{-2}). \tag{92}$$

For the matter variables one finds

$$\rho_*=O(r^{-5}), \tag{93}$$

$$e=O(r^{-1}), \tag{94}$$

$$p=O(r^{-6}), \tag{95}$$

$$v^u=1+2c/r+(2c^2-ac)/r^2+O(r^{-3}), \tag{96}$$

$$\tilde{v^a}=0 \quad \text{otherwise.} \tag{97}$$

In terms of the numerical evolution the important point to note is the fact that β vanishes to third order at null infinity despite the presence of matter. We are therefore still able to use the boundary condition $\beta=0$ at null infinity in this more general setting.

VI. NUMERICAL METHODS

The equations are discretized using finite-difference methods which are accurate to second-order in the grid space and time intervals. The evolution equations (4)–(6) for D, E and Z (represented by $\mathcal{U}$ below) can be written in the form

$$\frac{\partial}{\partial t}\mathcal{U}(r,t)+\frac{1}{r^2}\frac{\partial}{\partial r}[r^2\mathcal{F}(r,t;\mathcal{U},a,\alpha)]+\mathcal{S}(r,t;\mathcal{U},a,\alpha)=0, \tag{98}$$

which can also be written as

$$\frac{\partial \mathcal{U}}{\partial t}+3\frac{\partial}{\partial r^3}(r^2\mathcal{F})+\mathcal{S}=0. \tag{99}$$

The discrete form of Eq. (99) has improved behavior near $r=0$. The equation is differenced using a two-step, predictor-corrector MacCormack scheme [13],

$$\tilde{\mathcal{U}}_i=\mathcal{U}_i^n-\frac{3\Delta t}{r_{i+1}^3-r_i^3}(r_{i+1}^2\mathcal{F}_{i+1}^n-r_i^2\mathcal{F}_i^n)-\Delta t\mathcal{S}_i^n, \tag{100}$$

where $\mathcal{X}_i^n=\mathcal{X}(r_i,t^n)$. Once all the predicted values $\tilde{\mathcal{U}}$ have been found, the metric variables a and α must also be predicted using the methods described below. The corrected values of the fluid quantities are, then,

$$\mathcal{U}_i^{n+1}=1/2(\tilde{\mathcal{U}}_i+\mathcal{U}_i^n)-\frac{3/2\Delta t}{r_i^3-r_{i-1}^3}(r_i^2\tilde{\mathcal{F}}_i-r_{i-1}^2\tilde{\mathcal{F}}_{i-1}) -1/2\Delta t\tilde{\mathcal{S}}_i. \tag{101}$$

Near $r=0$ the variables D and E are expanded as even functions, e.g.

$$D(r\to 0)=A+Br^2, \tag{102}$$

where the time-dependent coefficients A and B are determined using interior values of D. The quantity Z is an odd function and at $r=0$ we have $Z=0$.

On the characteristic side the evolution equations (37)–(39) for the $\mathcal{U}=\{\rho_*,e,v^u\}$ variables can be written in the non-conservative form

$$\frac{\partial \mathcal{U}}{\partial u}+\mathcal{A}\frac{\partial \mathcal{U}}{\partial y}+\mathcal{S}=0, \tag{103}$$

where $\mathcal{S}$ may contain spatial derivatives of the other variables. It is simple to modify the MacCormack difference scheme for this type of equation. At the interface the relationships listed in Appendix B are used to obtain difference formulas which express Cauchy quantities and their radial derivatives in terms of characteristic quantities, and vice versa. This enables us to continue the Cauchy and characteristic integrations through the interface in both directions. Note that some of the relationships involve t and u derivatives: hence more than one time level is required to obtain some of the difference formulas.

It is not possible to have values of $D=E=p=\rho_*=e=0$ anywhere on the grid since it would then be impossible to solve Eq. (14) and some type of fluid-vacuum interface tracking would be required. To avoid this complication every grid point has at least a ''vacuum'' level of these variables [8]. Typically the ''vacuum'' level is around 10^{-10} times that of the peak value of the variable in the initial data set.

Because the evolution equations (4)–(6) and (37)–(39) are non-linear and are propagating waves in a compressible fluid, it is highly likely that shocks and other discontinuities will occur. It is well known that second-order accurate dis-

cretizations of such equations produce spurious oscillations at shock fronts and require some form of artificial dissipation to reduce the effect. A highly satisfactory solution is to use so-called *high-order Godunov* methods along with flux-limiters, usually of the total variation diminishing (TVD) type. These have recently been used for spherical general relativistic flows where they are far more accurate than standard artificial viscosity when the flow velocities are very close to the speed of light [14]. The main problem with such schemes is their complexity. For the work considered in this paper the flow velocities are kept to values typically less than 80% of the speed of light. Furthermore, their implementation with CCM has yet to be investigated. Thus the advantages of the high-order Godunov schemes are less appealing for the work considered here. Here we use a second-order viscous term (described below) to dissipate solutions of Eqs. (4)–(6) and (37)–(39) near steep gradients. An additional problem which can be solved by artificial dissipation arises due to the ''vacuum'' levels of the variables at certain points on the grid, as described previously. The fluid has a very low density, but can have a significant velocity. This gives rise to a noisy evolution, which, if left unchecked, can begin to dominate the numerical solution due to erratic behavior in the 3-velocity. A small amount of dissipation can eliminate this problem very effectively.

Once the quantities $\mathcal{U}$ have been evaluated at the new time level, they are dissipated according to the formula

$$\mathcal{U}_i^{n+1}=\mathcal{U}_i^{n+1}+\eta_i(\mathcal{U}_{i+1}^n-\mathcal{U}_i^u)-\eta_{i-1}(\mathcal{U}_i^n-\mathcal{U}_{i-1}^n) \tag{104}$$

where the dissipation coefficient, η, is calculated in the following way:

$$\begin{aligned}\max\{\ln(E_{vac}/\tilde{E}_{max}),\min[0,\ln(\tilde{E}/\tilde{E}_{max})]/\ln(E_{vac}/\tilde{E}_{max})\}&=\xi,\\ \min(\xi,1)^6&=\xi^*,\\ 1/16(1-\xi^*)+\xi^*&=\xi^{**}.\end{aligned} \tag{105}$$

In the above E_{vac} is the ''vacuum'' level of E set at the start of the evolution and $\tilde{E}_{max}$ is the maximum value of $\tilde{E}$ on the current time slice. Note that the predicted values of E are used. Then

$$\eta=1/3\xi^{**}(1/2+\epsilon^2), \tag{106}$$

where

$$\epsilon=\frac{\Delta t}{\Delta r}V^r \tag{107}$$

for the D and Z variables, while

$$\epsilon=\frac{\Delta t}{\Delta r}\left(\frac{E+p}{E}\right)V^r \tag{108}$$

for the E variable. The property of expression (105) is such that $\xi^{**}\approx 1$ when $\tilde{E}\approx E_{vac}$ and $\xi^{**}\approx 1/16$ otherwise. The large power in ξ^* ensures that ξ^{**} moves rapidly away from 1 and towards 1/16 as $\tilde{E}$ increases above E_{vac}. Analogous expressions may be obtained for the characteristic equations with e used in place of E.

Both of the radial constraint equations (7) and (8) on the Cauchy side can be written in the form

$$\frac{d}{dr}\ln\mathcal{A}(r)=\mathcal{Y}(r;U,a), \tag{109}$$

where $\mathcal{A}$ represents α or a and importantly $\mathcal{Y}$ is independent of α, but dependent upon a. This equation can be differenced to second order accuracy in space as

$$\ln\mathcal{A}_{i+1}-\ln\mathcal{A}_i=1/2\Delta r(\mathcal{Y}_{i+1}+\mathcal{Y}_i), \tag{110}$$

where $\Delta r=r_{i+1}-r_i$. The solution for a requires iteration of the discrete equation

$$a_{i+1}=a_i\exp[1/2\Delta r(\mathcal{Y}_{i+1}+\mathcal{Y}_i)] \tag{111}$$

with a starting value $a=1$ at $r=0$. By contrast the lapse is found algebraically from

$$\alpha_i=\alpha_{i+1}\exp[-1/2\Delta r(\mathcal{Y}_{i+1}+\mathcal{Y}_i)], \tag{112}$$

where the outer starting value of α is obtained from the characteristic portion of the spacetime as described below. Since α is an even function of r, it is expanded near $r=0$ as in Eq. (102). The radial equations (33)–(35) on the characteristic side are straightforward to difference, but they must be integrated in the correct order and the right direction (inwards or outwards). The integration scheme, in outline, consists of the following. Given a distribution of D, E, Z on the Cauchy side and ρ_*, e, v^u on the characteristic side, either from an initial data set or a previous evolution, we first integrate Eq. (8) for a outwards from $r=0$ to the interface $r=r_0$. Next we integrate Eq. (33) for β inwards from $y=0$ to the interface $y=y_0=1/r_0$. The boundary condition is $\beta(y=0)=0$ provided the asymptotic matter distribution is as described in Sec. V. From relationship (B12) it is then possible to obtain a starting value for α at the interface so that Eq. (7) can be integrated inwards from $r=r_0$ to $r=0$. In addition, from Eq. (B13) a starting value for W can be found to enable the integration of Eq. (34) outwards from $y=y_0$ to $y=0$. Once β and W have been found, it is straightforward to integrate Eq.

(35) inwards to obtain $\mathcal{B}$. The boundary condition is $\mathcal{B}(y=0)=0$, again valid when the asymptotic fluid behavior is as described in Sec. V. Afterwards Eqs. (4)–(6) and (37)–(39) are used to update the fluid variables. The whole process is then repeated to continue the evolution.

VII. RESULTS

We have investigated two general scenarios with the combined code. The first describes configurations where the fluid flow is predominately outwards, crossing the interface from the Cauchy region into the characteristic region. In the second case the initial conditions are arranged so that the fluid collapses inwards, leading to black hole formation. In addition we investigate the stability and convergence behavior of the code.

A. Outflow

The initial data consist of specifying the density and velocity profiles of the fluid. To determine the initial pressure we use the relationship

$$p=K\rho_*^{\Gamma}, \tag{113}$$

which is consistent with the adiabatic equation of state (9). Here K is a constant which controls the initial specific internal energy, e, of the fluid. We then solve Eq. (8) for a, Eq. (33) for β, Eq. (7) for α and Eq. (34) for W in the manner described at the end of Sec. VI. For simplicity we choose the initial 3-velocity to be zero everywhere. The density profile must be chosen such that it satisfies $\partial\rho_*/\partial r=0$ at $r=0$ and must fall off asymptotically like the Buchdahl solution as described in Sec. V. We satisfy these requirements by using a Gaussian profile near $r=0$ and an asymptotic Buchdahl solution attached at some patching radius r_P. The Gaussian profile is given by

$$\rho_{*G}(r)=\rho_{*M}\,\exp(-r^2/\sigma^2), \tag{114}$$

where ρ_{*M} is the maximum density at $r=0$ and σ determines the width of the Gaussian. At radius r_P we attach the profile

$$\rho_{*B}(r)=\frac{\rho_{*M}r_P^5}{r^6}\left\{\left[2\left(\frac{r_P}{\sigma}\right)^2-5\right]r_P-\left[2\left(\frac{r_P}{\sigma}\right)^2-6\right]r\right\}\times\exp(-r_P^2/\sigma^2). \tag{115}$$

It can be seen that, at the patching radius r_P,

$$\rho_{*G}=\rho_{*B}=\rho_{*M}\,\exp(-r_P^2/\sigma^2), \tag{116}$$

$$\rho'_{*G}=\rho'_{*B}=-2\rho_{*M}\left(\frac{r_P}{\sigma^2}\right)\exp(-r_P^2/\sigma^2). \tag{117}$$

Moreover, in the limit of large r,

$$\rho_{*B}\sim A/r^5, \tag{118}$$

where

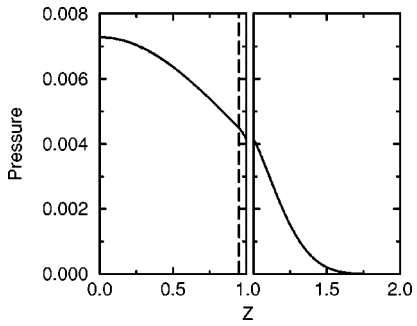

FIG. 1. The pressure profile at time $t=0$. The radial coordinate z is defined by Eq. (120). The interface is placed at $z=1$ and future null infinity is at $z=2$. The Buchdahl solution is patched onto the Gaussian profile at $z=0.95$, denoted by the dashed line.

$$A=\rho_{*M}r_P^5\left[6-2\left(\frac{r_P}{\sigma}\right)^2\right]\exp(-r_P^2/\sigma^2). \tag{119}$$

The free parameters specifying the initial data are then ρ_{*M}, K, Γ, σ and r_P. In order for A to be positive we should have $\sigma>r_P/\sqrt{3}$. Note that in the characteristic region the substitution $r=1/y$ is used in Eq. (115) which remains well-behaved in the limit $y\to 0$.

We have performed many runs with the code. A typical initial pressure profile which gives rise to outflow is shown in Fig. 1. The chosen values are $\rho_{*M}=2\times10^{-4}$, $K=200$ and $\sigma=1.5$ with $\Gamma=6/5$ as required by the Buchdahl solution. The Cauchy-characteristic interface is kept fixed at $r_0=1$ and $r_P=0.95$ for all runs of the code. If we were to take $r_0=10^6$ cm, which is the radius of a typical neutron star, then the central density value would correspond to $\approx 2.7\times10^{12}$ g cm^{-3}, indicating dense relativistic matter. The ADM mass in geometric units is $M=0.3$, which equates to around 4×10^{33} g or $2M_\odot$. This configuration is quite relativistic, having a central lapse value $\alpha_c=0.64$. Note that the width of the Gaussian is somewhat larger than the radius of the Cauchy region which results in quite a large density at the interface. This will show that the technique allows for a small Cauchy region even when a significant amount of matter is present. It is important that this be the case since CCM allows for gravitational wave extraction close to the source.

A convergence check on the code has been performed and the results are shown in Fig. 2. This shows the L_1 norm in the error of the metric function a for low ($N=151$), medium ($N=301$) and high ($N=601$) resolution runs of the initial data shown in Fig. 1. The reference solution has $N=1201$ grid points. The code exhibits 2nd-order convergence behavior, but note that for these initial conditions almost all of the fluid has moved off the Cauchy portion of the grid by $20M$ (where M is the ADM mass of the configuration) and the code is evolving very low densities. Figures 3(a), 3(b) and 3(c) show the evolution of the pressure p, the metric function a and the radial component of the 4-velocity v^r respectively. Since the particular relationships between these Cauchy quantities and the characteristic ones are valid for all r, and not just at the interface (see Sec. IV and Appendix B), it is possible to plot them using a radial coordinate z defined by

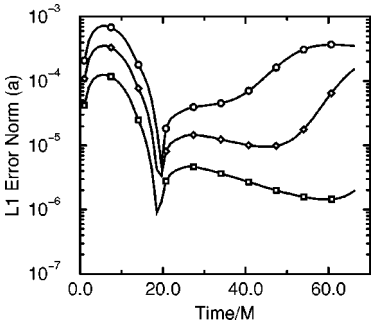

FIG. 2. Convergence behaviour of the CCM code. The L_1 error norm of the metric function a is shown for runs with grid resolutions of $N=151$ (open circles), $N=301$ (open diamonds) and $N=601$ (open squares). The reference solution has $N=1201$ grid points. Convergence is 2nd-order up to $t\approx 20M$ after which the code evolves very low densities and increased resolution generally shows better than 2nd-order convergence.

$$z=\begin{cases} r & \text{for } 0\leqslant r\leqslant 1 \\ 2-y & \text{for } 0\leqslant y\leqslant 1. \end{cases} \tag{120}$$

This means there is a change of coordinate systems from radial-polar to Bondi at $z=1$ and future null infinity is located at $z=2$. The figures have a break at the interface $r=1$. Note that the grid resolution is increased towards $r=0$ for improved accuracy. Figure 3(a) shows that after an initial inwards collapse the fluid moves smoothly out across the interface. The metric function a drops towards 1 everywhere in the Cauchy region as the fluid moves out. Note that the velocity component can become quite large in the low density characteristic region. Its value can be greater than 1, but of course the local 3-velocity of the fluid, $V^r=v^r/v^t$, is always less than 1. This type of configuration will run indefinitely.

B. Black hole formation

To obtain a black hole solution we begin with the same initial data as shown in Fig. 1, but modify the pressure profile while keeping the rest mass density constant, e.g.

$$p=\beta K\rho_*^{\Gamma}. \tag{121}$$

The results from a run with $\beta=2$ are shown in Figs. 4(a)–4(c). The total mass-energy of the configuration is increased, resulting in the formation of a black hole. In the radial-polar gauge the formation of a black hole is indicated by a rapid increase of the metric function a and a corresponding rapid decrease of the lapse α. In spherical symmetry the peak of a asymptotically approaches the horizon and therefore the radius of the black hole can be approximated. Here the black hole radius is $r_{BH}=0.87$ which is not far from the interface at $r_0=1$. In the asymptotic region the solution is once again an outflow as can be seen in Fig. 4(c). Note that the time-step is reduced as the black hole forms to maintain accuracy. This can be seen in the surface plots as the lines become closer in the time direction. The configuration evolves to about $13M$, after which the rapid increase in a halts the code.

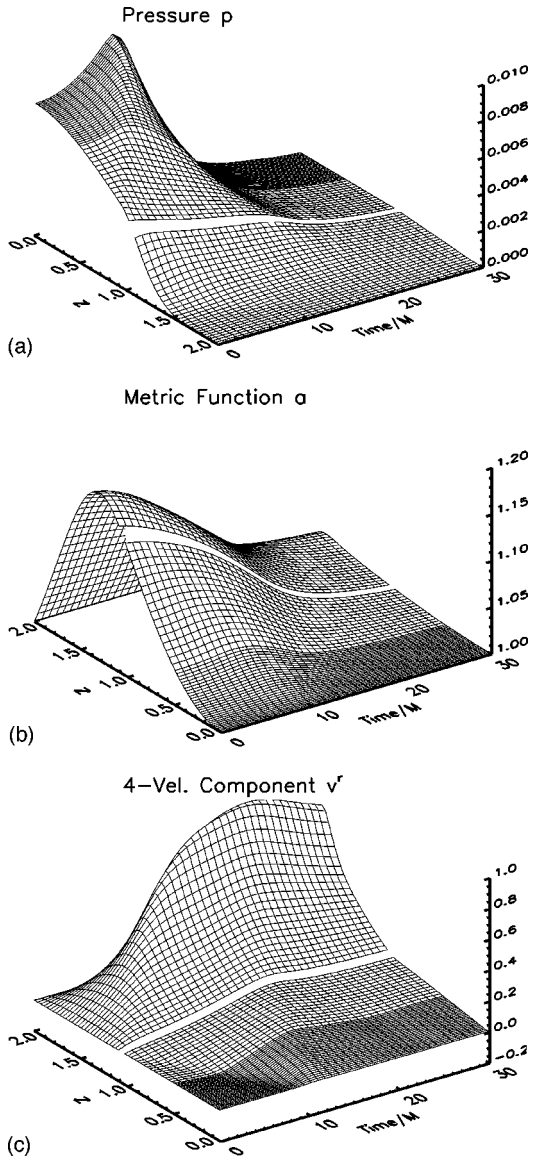

FIG. 3. Time evolution of mass outflow initial data showing (a) the pressure, (b) the metric function a, and (c) the v^r component of the fluid 4-velocity. Note that for clarity the z-axis is reversed for (a).

VIII. DISCUSSION

The work presented in this paper shows that the CCM technique can be applied effectively to perfect fluid spacetimes. Since in non-symmetrical situations it is very difficult to follow the fluid-vacuum interface, the approach adopted here has been to replace the vacuum region by one of very low density material [8]. The initial fluid distribution is described by a Gaussian pulse, while the low density exterior region is initially taken to be asymptotic to the finite mass static solution of Buchdahl.

The code is shown to be second order convergent and to be stable over long periods. There is no problem evolving the motion of the fluid until either it has moved off the Cauchy portion of the grid (and the code is then evolving the residual low density fluid) or until a black hole has formed. Further-

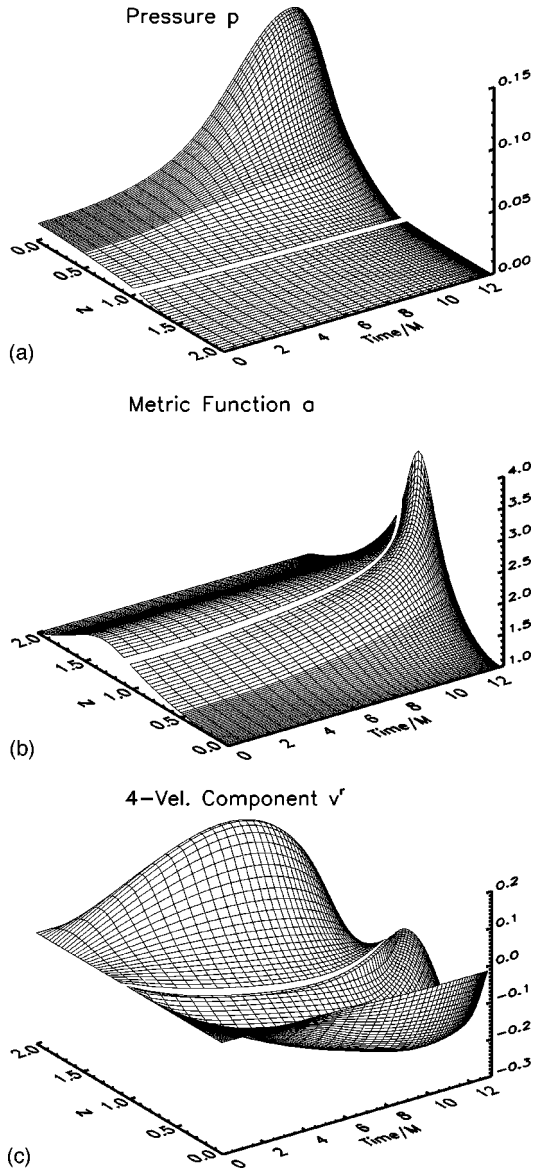

FIG. 4. Time evolution of initial data forming a black hole showing (a) the pressure, (b) the metric function a, and (c) the v^r component of the fluid 4-velocity. Black hole hole formation is indicated by a steep increase in a. Note that for clarity the z-axis is reversed for (a).

more, there appear to be no significant discontinuities of the variables or their derivatives either at the interface or the junction between the fluid and the background.

One of the problems of dealing with the fluid-vacuum interface by replacing it with a low density background when using a traditional $3+1$ code is that it involves the use of outer boundary conditions at the edge of the grid. These must deal with the inflow and outflow of matter as well as ensuring outgoing gravitational radiation. Such a procedure can be very problematic, especially in the case of significant inflow. To minimize these problems the Cauchy grid has to be taken to be very large, extending well beyond the boundary of the star, so that the boundary conditions can be applied in a region of very low density. A significant advantage in using CCM is the avoidance of having to apply such a boundary condition. This allows the Cauchy region to be quite small and it is shown in this paper that there is no problem locating the interface in a region where there is a significant fluid density. This shows the viability of using CCM to extract gravitational wave information from a small Cauchy region.

ACKNOWLEDGMENTS

This work has been supported by PPARC grant number GR/K44510.

APPENDIX A: SPHERICALLY SYMMETRIC FORM OF BONDI'S LINE ELEMENT

The solution of Killing's equations

$$L_{\mu\nu}=L_X g_{\mu\nu}=g_{\mu\nu,\sigma}X^\sigma+g_{\mu\sigma}X^\sigma_{,\nu}+g_{\nu\sigma}X^\sigma_{,\mu}=0 \quad \text{(A1)}$$

for the unit sphere

$$ds^2=d\theta^2+\sin^2\,\theta d\phi^2 \quad \text{(A2)}$$

in canonical spherical coordinates (θ,ϕ) is given by the three rotations

$$\cos\,\phi\frac{\partial}{\partial\theta}-\sin\,\phi\,\cot\,\theta\frac{\partial}{\partial\phi}=X_1, \quad \text{(A3)}$$

$$\sin\,\phi\frac{\partial}{\partial\theta}+\cos\,\phi\,\cot\,\theta\frac{\partial}{\partial\phi}=X_2, \quad \text{(A4)}$$

$$\frac{\partial}{\partial\phi}=X_3. \quad \text{(A5)}$$

The Bondi line element (15) already possesses X_3 as a Killing vector since it is axially symmetric. The condition that X_1 be a Killing vector from Eq. (A1) results in the following requirements

$$L_{00}=0\Rightarrow V_{,\theta}=0, \quad \text{(A6)}$$

$$L_{01}=0\Rightarrow \beta_{,\theta}=0, \quad \text{(A7)}$$

$$L_{02}=0\Rightarrow U_{,\theta}=0, \quad \text{(A8)}$$

$$L_{23}=0\Rightarrow \gamma=0. \quad \text{(A9)}$$

These conditions result in X_2 automatically being a Killing vector. Finally, using the requirement in spherical symmetry of invariance under the discrete reflection

$$\theta\rightarrow\pi-\theta, \quad \text{(A10)}$$

we find that

$$U=0. \quad \text{(A11)}$$

Thus the spherically symmetric form of Bondi's line element is

$$ds^2 = -\frac{Ve^{2\beta}}{\tilde{r}}du^2 - 2e^{2\beta}du\,d\tilde{r} + \tilde{r}^2 d\theta^2 + \tilde{r}^2 \sin^2\theta\, d\phi^2, \tag{A12}$$

where $V = V(u,\tilde{r})$ and $\beta = \beta(u,\tilde{r})$ only.

APPENDIX B: RELATIONSHIPS FOR INTERFACE MATCHING

We list here all the relationships required to obtain Cauchy quantities and their first radial derivatives in terms of characteristic quantities at the interface, and vice versa.

Cauchy variables in terms of Bondi variables:

$$A^{1/2} = \alpha, \tag{B1}$$

$$BA^{-1/2} = a, \tag{B2}$$

$$-[y^2 A_{,y}^{1/2} + (BA^{-1/2})_{,u}] = \alpha_{,r}, \tag{B3}$$

$$-[y^2 (BA^{-1/2})_{,y} + BA^{-1}(BA^{-1/2})_{,u}] = a_{,r}, \tag{B4}$$

$$v^{\tilde{r}} = v^r, \tag{B5}$$

$$v^u + BA^{-1}v^{\tilde{r}} = v^t, \tag{B6}$$

$$-[y^2 v^{\tilde{r}}_{,y} + BA^{-1}v^{\tilde{r}}_{,u}] = v^r_{,r}, \tag{B7}$$

$$-[y^2 v^u_{,y} + BA^{-1}(y^2 v^{\tilde{r}}_{,y} - v^u_{,u}) + B^2 A^{-2} v^{\tilde{r}}_{,u} + y^2 (BA^{-1})_{,y} v^{\tilde{r}} - (BA^{-1})_{,u} v^u] = v^t_{,r}, \tag{B8}$$

$$-[y^2 \Phi_{,y} + BA^{-1}\Phi_{,u}] = \Phi_{,r}, \tag{B9}$$

where

$$A = e^{2\beta}(yW + e^{2\beta}), \tag{B10}$$

$$B = e^{2\beta}, \tag{B11}$$

the scalars $\Phi = \{\rho_*, e\}$, and $v^{\tilde{r}}$ can be obtained from the normalization condition (18). Note that the relations (B2) and (B5) are valid for all r and not just at the interface. Bondi variables in terms of Cauchy quantities:

$$\frac{1}{2}\ln(\alpha a) = \beta, \tag{B12}$$

$$\alpha a^{-1} r(1-a^2) = W, \tag{B13}$$

$$-r^2\Big[(a\alpha^{-1})_{,t} + \frac{1}{2}\alpha a^{-1}(a\alpha^{-1})^{,r} + \alpha^{-1}\alpha_{,r} + a\alpha^{-2}\alpha_{,t}\Big] = \beta_{,y}, \tag{B14}$$

$$-\alpha a^{-1} r(1-a^2) + r^2[2a\alpha(a\alpha^{-1})_{,t} + (1+a^{-2})\alpha^2(a\alpha^{-1})_{,r} + 2a\alpha_{,r} + 2a^2\alpha^{-1}\alpha_{,t}] = W_{,y}, \tag{B15}$$

$$v^r = v^{\tilde{r}}, \tag{B16}$$

$$v^t - a\alpha^{-1}v^r = v^u, \tag{B17}$$

$$-r^2[v^r_{,r} + a\alpha^{-1}v^r_{,t}] = v^{\tilde{r}}_{,y}, \tag{B18}$$

$$-r^2[v^t_{,r} - v^t(a\alpha^{-1})_{,t} - v^r(a\alpha^{-1})_{,r} + a\alpha^{-1}(v^t_{,t} - v^r_{,r}) - \alpha^2 a^{-2} v^r_{,t}] = v^u_{,y}, \tag{B19}$$

$$-r^2[\Phi_{,r} + a\alpha^{-1}\Phi_{,t}] = \Phi_{,y}, \tag{B20}$$

where again the scalar $\Phi = \{\rho_*, e\}$.

[1] J. Winicour, ''Characteristic Evolution and Matching'' (Living Reviews: Web address http://www.livingreviews.org, 1998).

[2] N. T. Bishop, in *Approaches to Numerical Relativity*, edited by R. A. d'Inverno (Cambridge University Press, Cambridge, England, 1992), pp. 20–33; N. T. Bishop, Class. Quantum Grav. **10**, 333 (1993); R. Gómez, P. Laguna, P. Papadopoulos and J. Winicour, Phys. Rev. D **54**, 4719 (1996); N. T. Bishop, R. Gómez, L. Lehner and J. Winicour, *ibid.* **54**, 6153 (1996); N. T. Bishop, R. Gómez, P. R. Holvorcem, R. A. Matzner, P. Papadopoulos and J. Winicour, Phys. Rev. Lett. **76**, 4303 (1996); N. T. Bishop, R. Gómez, P. R. Holvorcem, R. A. Matzner, P. Papadopoulos and J. Winicour, J. Comput. Phys. **136**, 140 (1997); P. Papadopoulos and P. Laguna, Phys. Rev. D **55**, 2038 (1997); N. T. Bishop, R. Gómez, L. Lehner, M. Maharaj and J. Winicour, *ibid.* **56**, 6298 (1997); R. Gómez, R. Marsa and J. Winicour, *ibid.* **56**, 6310 (1997).

[3] C. J. S. Clarke, R. A. d'Inverno and J. A. Vickers, Phys. Rev. D **52**, 6863 (1995); M. R. Dubal, R. A. d'Inverno and C. J. S. Clarke, *ibid.* **52**, 6868 (1995).

[4] R. A. d'Inverno and J. A. Vickers, Phys. Rev. D **54**, 4919 (1996); R. A. d'Inverno and J. A. Vickers, *ibid.* **56**, 772 (1997).

[5] N. T. Bishop and P. Haines, Quaest. Math. **19**, 259 (1996).

[6] R. S. Hamadé, Ph.D. thesis, University of Cambridge, 1996.

[7] S. L. Shapiro and S. A. Teukolsky, Astrophys. J. **298**, 34 (1985); S. L. Shapiro and S. A. Teukolsky, Astrophys. J. **298**, 58 (1985); M. R. Dubal, Class. Quantum Grav. **8**, 453 (1991); P. J. Mann, J. Comput. Phys. **107**, 188 (1993); P. Laguna, W. A. Miller and W. H. Zurek, Astrophys. J. **404**, 678 (1993); F. A. Raiso and S. L. Shapiro, *ibid.* **438**, 887 (1995); J. C. Charlton and P. Laguna, *ibid.* **444**, 193 (1995).

[8] R. F. Stark and T. Piran, Comput. Phys. Rep. **5**, 221 (1987); K. Oohara and T. Nakamura, Prog. Theor. Phys. **88**, 1079 (1992); M. Shibata, T. Nakamura and K. Oohara, *ibid.* **89**, 809 (1993).

[9] R. Arnowitt, S. Deser, and C. W. Misner, in *Gravitation: An Introduction to Current Research*, edited by L. Witten (Wiley, New York, 1962), p. 227; J. W. York, in *Sources of Gravitational Radiation*, edited by L. Smarr (Cambridge University

Press, Cambridge, England, 1979), pp. 83–126.
[10] J. M. Bardeen and T. Piran, Phys. Rep. **96**, 205 (1983).
[11] H. Bondi, M. G. J. van der Burg and A. W. K. Metzner, Proc. R. Soc. London **A269**, 21 (1962).
[12] H. A. Buchdahl, Astrophys. J. **140**, 1512 (1964).
[13] C. A. J. Fletcher, *Computational Techniques for Fluid Dynamics* (Springer-Verlag, Berlin, 1991), Vol. II.
[14] J. M. Martí, J. M. Ibáñez and J. A. Miralles, Phys. Rev. D **43**, 3794 (1991); J. M. Ibáñez, J. M. Martí, J. A. Miralles and J. V. Romero, in *Approaches to Numerical Relativity*, edited by R. A. d'Inverno (Cambridge University Press, Cambridge, England, 1992), pp. 223–229; J. V. Romero, J. M. Ibáñez, J. M. Martí and J. A. Miralles, Astrophys. J. **462**, 839 (1996); F. Banyuls, J. A. Font, J. M. Ibáñez, J. M. Martí and J. A. Miralles, *ibid.* **476**, 221 (1997); L. Q. Wen, A. Panaitescu and P. Laguna, *ibid.* **486**, 919 (1997).